JOURNAL OF CATALYSIS 148, 252–260 (1994)

Formation of 2,3-Pentanedione from Lactic Acid over Supported Phosphate Catalysts

Garry C. Gunter,* Dennis J. Miller,*,[1] and James E. Jackson†

*Department of Chemical Engineering and †Department of Chemistry, Michigan State University, East Lansing, Michigan 48824

Received December 7, 1993; revised February 24, 1994

Lactic acid is converted to 2,3-pentanedione, acrylic acid, and acetaldehyde in vapor-phase reactions at 0.5 MPa over phosphate salts. Highest selectivities to 2,3-pentanedione are achieved at 280–300°C and long (2–4 sec) residence times, while selectivity to acrylic acid is best at 350°C and short residence times (0.4 sec). 2,3-Pentanedione is proposed to form by a second-order condensation in the presence of phosphate, while acrylic acid is proposed to result from elimination of water via a cyclic lactic acid–phosphate transition state.

INTRODUCTION

Lactic acid (2-hydroxy-propanoic acid) is a bifunctional, optically active molecule traditionally used in limited quantities (40–50 million lb/year) as a food additive and in textile production. It is undergoing a surge in production via efficient starch-based fermentation processes, with potential applications in biodegradable polylactide polymers (1, 2). Decreased cost associated with these new production technologies suggests that lactic acid could become a major biomass-based feedstock in the near future.

In this paper, reactions of vapor-phase lactic acid over supported phosphate salts are investigated. In addition to previously documented (3, 4) pathways of lactic acid conversion to acrylic acid and acetaldehyde, we report for the first time the formation of 2,3-pentanedione as a major product of lactic acid conversion. This high-value fine chemical is currently produced in limited quantities ($\sim 4 \times 10^3$ kg/year) through a multistep chemical synthesis or via recovery from dairy waste. It is used primarily as a flavoring ingredient but has potential for applications as a feedstock (5), solvent (6), or photoinitiator for radical chain reactions (7).

Primary pathways of lactic acid conversion are shown in Fig. 1. Direct dehydration of lactic acid to acrylic acid has long been of interest as a potential route to polymers from biomass, and most lactic acid conversion studies have focused on this reaction. Holmen (4) first reported the conversion over sulfate and phosphate catalysts in 1958, achieving acrylic acid yields of 68% over Na_2SO_4 at 400°C. Paparizos *et al.* (8) report a 61% yield of acrylic acid from ammonium lactate at 340°C and 4.2-sec residence time over NH_3-treated $AlPO_4$. With lactic acid as the feed, the best acrylic yield was 43% at 340°C. Sawicki (9) reported an acrylic acid yield of 58% with a selectivity of 65% at 350°C, using silica-supported NaH_2PO_4 buffered with $NaHCO_3$. Recently, researchers at Batelle reported (10) development of a process for converting methyl lactate to methyl acrylate over $CaSO_4$, but no yield information was given.

High acrylate yields can be obtained over phosphate catalysts from compounds similar in structure to lactic acid. For instance, 64% butyl methacrylate was obtained from butyl-2-methyl-2-hydroxypropanoate over Ca–Mg phosphate (11). Also, 87.5% methyl methacrylate was obtained from 2-hydroxyisobutyramide (in methanol) over NH_3-treated YPO_4 (12).

As can be seen, phosphates are active catalysts for dehydration of lactic acid and related compounds. In general, the activity of phosphate salts as catalysts is well known (13), particularly for dehydration of alcohols (14). For dehydration of α-hydroxy carboxylic acids such as lactic acid, studies using phosphate esters (15) or hydroxyisobutyric acid (16, 17) suggest that the phosphate stabilizes the carboxylate group, thus preventing decarboxylation. At this time, however, the mechanism by which prosphates catalyze dehydration is not known.

Reactions of lactic acid in supercritical water are reported by Mok *et al.* (18). In addition to primary conversion pathways to acrylic acid and acetaldehyde, secondary pathways identified include acetic acid and acetone from acetaldehyde, hydrogenation of acrylic acid to propanoic acid, and decarboxylation of acrylic acid to ethene. The best acrylic acid yields (23%) were achieved in slightly basic solutions. Lira and McCrackin (19) studied lactic acid dehydration in near critical water using phosphates as catalysts. They achieved 58% selectivity to

[1] To whom correspondence should be addressed.

0021-9517/94 $6.00

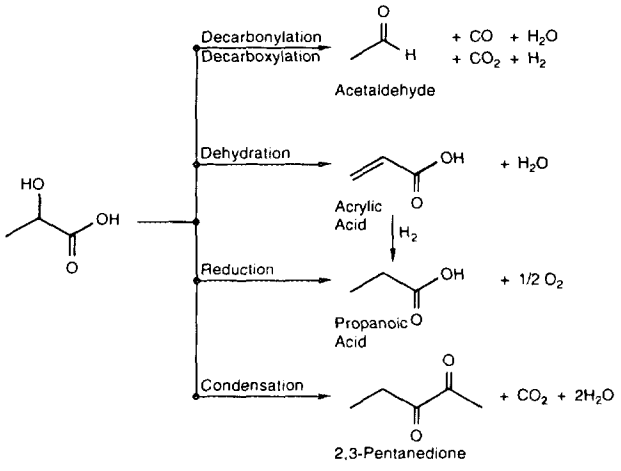

FIG. 1. Primary conversion pathways of lactic acid.

acrylic acid from a solution of 0.4 *M* lactic acid and 0.1 *M* sodium phosphate at a pressure of 310 bars and 360°C.

Formation of acrylates from lactates via pyrolysis of the intermediate α-acetoxypropionate was first described by Burns *et al.* (20). This intermediate, formed by reaction of methyl lactate with acetic anhydride, can be converted to methyl acrylate in yields as high as 90% (21) at 550°C and 10 sec contact time over nonporous contact materials such as quartz. The chemical attractiveness of this pathway is unfortunately offset by the high cost of regenerating acetic anhydride.

METHODS

Reactants and Standards

Lactic acid feed (Aldrich, 85 wt%) was diluted to 34 wt% to simulate a typical refined lactic acid fermentation product. Higher feed concentrations led to incomplete vaporization and plugging of the feed line, and lower concentrations gave lower product formation rates. The feed concentration of lactic acid was verified by C–H–N elemental analysis. High purity helium (AGA, 99.99%) was used as a carrier gas. High purity acrylic acid, 2,3-pentanedione, propanoic acid, acetaldehyde, hydroxyacetone, and other chemicals were used as calibration standards.

Catalyst Preparation and Characterization

Sodium phosphate salts ($NaH_2PO_4 \cdot H_2O$, $Na_2HPO_4 \cdot H_2O$, $Na_3PO_4 \cdot 12H_2O$, Aldrich) were deposited onto a low surface area silica–alumina support by wet impregnation and drying for 24 hr at 100°C. The support (93% Al_2O_3, 7% SiO_2, Johnson–Matthey) has a surface area of 5 m^2/g as measured by N_2 BET analysis; as-received support pellets (2-mm extrudate) were crushed and sieved to −16 + 30 mesh prior to impregnation. Unless noted otherwise, all catalyst loadings were 0.001 mol/g of support.

Monosodium and disodium phosphates undergo dehydration upon heating. Dehydration of NaH_2PO_4 to sodium acid pyrophosphate ($Na_2H_2P_2O_7$) occurs around 200°C, and further dehydration to linear or cyclic sodium metaphosphate $(NaPO_3)_n$ occurs at 260–300°C (22). Dehydration of Na_2HPO_4 to give sodium pyrophosphate ($Na_4P_2O_7$) occurs around 260°C (23). We conducted ^{31}P MAS NMR of supported sodium phosphate salts following heating to 300°C for 1 hr; the spectra obtained, upon comparison with literature spectra (24), indicate that NaH_2PO_4 and Na_2HPO_4 fully dehydrate upon heating to 300°C. The species present at the onset of reaction are therefore $(NaPO_3)_n$, $Na_4P_2O_7$, and Na_3PO_4 for the mono-, di-, and tribasic sodium phosphates, respectively.

Biomineral-derived calcium hydroxyapatite was also investigated on a limited basis as a potentially inexpensive phosphate catalyst. This catalyst was prepared by calcination of bovine teeth in air at 800°C for 4 hr to remove organic matter, and then crushed to −16 + 30 mesh. The N_2 BET surface area of the hydroxyapatite was 6 m^2/g following preparation. The MAS ^{31}P NMR spectrum of the prepared hydroxyapatite gave essentially a single peak, illustrating the homogeneity of the material.

Reactor Description

All reactions were performed in a vertical, down-flow packed bed reactor equipped with a quartz insert. The vertical, quartz-lined configuration was found preferable to other orientations: a horizontal reactor led to coking and poor product recovery as a result of incomplete lactic acid vaporization, and the use of a metal liner led to undesirable lactic acid conversion to acetaldehyde and propanoic acid.

A diagram of the reactor system is given in Fig. 2. The reactor body consists of a 316 stainless steel tube 19.5 in. long, 1.25 in. o.d. and 0.55 in. i.d. A flange closure at the bottom of the reactor, sealed by a spring-loaded metal seal (Helicoflex), facilitates internal access. The system is designed for pressures up to 5 MPa at a temperature of 500°C. The catalyst is supported on a coarse quartz frit fused into the 19-in.-long × 0.50-in.-i.d. quartz liner tube, which is inserted into the reactor from the bottom and sealed to the flange to prevent gas bypass. An intenal quartz thermocouple well extends from the reactor flange to the bottom of the support frit to measure reaction temperature.

The high-temperature zone of the reactor is heated by a clamshell electric heater controlled by a programmable temperature controller with an external control thermocouple. A 6.5-in.-long and 0.5-in.-thick copper heat sink

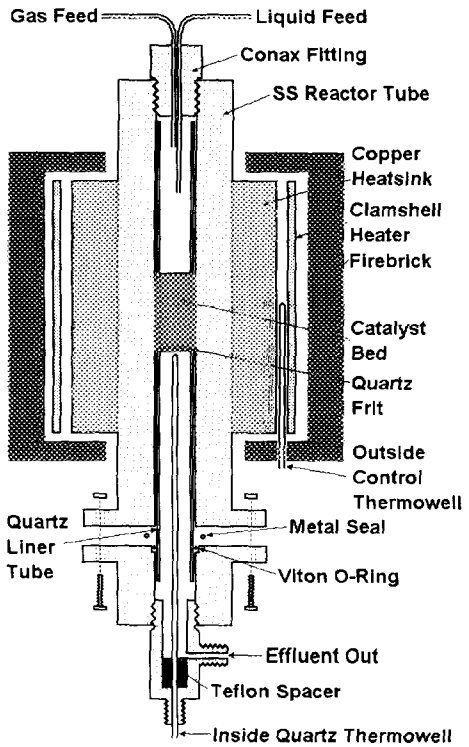

FIG. 2. Schematic of vapor-phase reactor.

surrounds the reactor in the heated zone to minimize temperature gradients. During operation, catalyst temperature is measured by the internal thermocouple, and reactor set point is adjusted to achieve the desired values. The reactor ends are heated by flexible heat tape to prevent product or lactic acid condensation.

Stainless steel liquid and gas feed tubes (0.062-in. o.d.) enter the top of the reactor through a Conax fitting and extend well inside the quartz liner tube. Liquid feed solutions are pumped with an Eldex HPLC metering pump, and helium is used as an inert to flush the reactor and dilute the feed during reaction.

Product Collection

Products of reaction exit the bottom of the reactor and pass first through a 10-ml stainless steel trap placed in an ice bath. Noncondensible products flow through a metering valve and a flowmeter and are collected in a gas collection bag. Typically, products are collected for a specified period of time (10–120 min) during steady-state operation of the reactor; the volume of liquid product and gas product collected is measured during steady-state operation in order to conduct an overall mass balance. During transient periods of operation, liquid products are condensed in a waste trap and gases are exhausted to a fume hood. All traps and exit lines are cleaned between each run.

Product Analysis

Analysis of condensible products is performed using a 4% Carbowax/Carbopack B-DA packed column in a Varian 3700 gas chromatograph with FID detection. Crude condensed effluent is filtered using disposable syringe filters to remove the small quantity of particulates present, then mixed with a solution containing 2-propanol as an internal standard and oxalic acid as a column conditioner. Good reproducibility of the lactic acid analysis is achieved by injecting 1-μl samples directly onto the column and leaving the syringe in the injector for 1 min. This assures complete lactic acid vaporization and results in linear calibration curves for lactic acid.

Major products analyzed include acrylic acid, propanoic acid, 2,3-pentanedione, acetaldehyde, and hydroxyacetone (acetol). Minor products include ethanol, acetone, acetic acid, methyl acetate, pyruvic acid, and several unknowns; together these minor products are reported as "Other" in the results. All product yields are calculated from ratios of product-to-internal standard peak areas and detector response factors. Product identification, particularly for 2,3-pentanedione, was conducted by matching of residence time with standards, by gas chromatography/mass spectroscopy, and by ^{1}H NMR.

Gas samples were analyzed using a Spherocarb column in a Perkin–Elmer 3400 gas chromatograph with thermal conductivity detection. Gas products analyzed include CO, CO_2, methane, ethane, ethylene, and acetylene. Yields of CO and CO_2 are reported as mole of gas per mole lactic acid fed.

Peak areas from GC analyses, liquid and gas product volumes, and feed flow rate and concentration are entered into a spreadsheet program which calculates product yields, selectivities, and the overall carbon mass balance for the experiment. Product yield is reported as a percentage of the theoretical yield based on lactic acid fed to the reactor; product selectivity is the percentage of theoretical yield based on lactic acid reacted to products. Typically, the overall carbon balance gives recoveries ranging from 85 to 105%; a more complete treatment of the carbon balance is given in the Discussion.

Procedure

Each catalyst loaded into the reactor is tested at several temperatures and residence times in a given experiment. The catalyst is first heated in helium until the temperature reaches 280°C, at which time lactic acid solution is fed at a relatively high flow rate (0.5 ml/min). Once product flow is established, helium and lactic acid solution flow rates are adjusted to desired values and the system is allowed to reach steady state. Reactor effluent is then directed to the product collection trap and gas bag for a specified time period of collection. The process is repeated at each

TABLE 1

Reaction Conditions

Temperature (°C)	250–375
Pressure (MPa)	0.5
Liquid flow rate (ml/min)	0.05–0.5
Helium flow rate (ml/min)	10–100
Feed composition (mole fraction)	Lactic acid: 0.08 Water vapor: 0.77 Helium: 0.15
Catalyst weight (g)	2.0–6.0
Catalyst bed height (cm)	2.5–7.6
Residence time (sec)	0.3–5.0

set of reaction conditions. A compilation of experimental conditions is given in Table 1.

RESULTS

Reaction Studies

Selected results of reaction studies over supported phosphate salts are reported here at different combinations of temperature and residence time. Residence time, calculated from actual feed rates and bed height, is the actual contact time of reactants with the catalyst. All experiments were conducted at 0.5 MPa absolute pressure using the feed composition given in Table 1. All key trends in activity and selectivity are represented in this paper; complete results are reported elsewhere (25).

Reaction studies were initially conducted to characterize thermal decomposition of lactic acid in the empty, quartz-lined reactor and over the Si/Al support. Representative results of experiments at 300 and 350°C (residence time = 0.3 sec) are given in Table 2. In the empty reactor, lactic acid conversion was less than 10% at 350°C; conversion over Si/Al support gives acetaldehyde as the dominant product.

The enhancement of acrylic acid and 2,3-pentanedione yields in the presence of disodium and trisodium phosphates is clearly demonstrated in Table 2. At 300°C, the trisodium salt shows a higher overall activity, but selectivities to various products are similar within experimental uncertainty for the two salts. At 350°C, both selectivities and overall activities are similar for di- and tribasic sodium phosphates. The monosodium salt exhibits little catalytic activity at either temperature. There is a fairly good (within ±20%) correlation between combined acetaldehyde and 2,3-pentanedione yields and combined CO and CO_2 yields, indicating that lactic acid is primarily reacting by pathways given in Fig. 1.

Yields of 2,3-pentanedione and acrylic acid over Na_3PO_4 on Si/Al are given as a function of residence time and temperature in Figs. 3 and 4, respectively. Clear maxima in product yield versus temperature are observed for both products. Selectivity to 2,3-pentanedione (43 ± 3%) is nearly independent of residence time at 280°C but declines with increasing residence time at higher temperatures, suggesting that secondary reaction is taking place.

TABLE 2

Product Yields and Selectivities[a] from Lactic Acid[b]

Temperature	300°C					350°C				
Substrate	None (empty reactor)	Support only	NaH_2PO_4	Na_2HPO_4	Na_3PO_4	None (empty reactor)	Support only	NaH_2PO_4	Na_2HPO_4	Na_3PO_4
Acrylic acid	0 (0)	0.1 (1)	0.1 (6)	0.6 (17)	2.0 (14)	0.1 (3)	0.8 (4)	1.5 (17)	9.7 (29)	9.8 (31)
2,3-Pentanedione	0 (0)	0.2 (3)	0.2 (11)	1.6 (44)	4.3 (31)	0 (0)	0.3 (2)	1.3 (15)	8.1 (24)	7.0 (22)
Acetaldehyde	0.1 (20)	1.5 (22)	0.4 (22)	0.7 (19)	1.9 (14)	1.5 (43)	9.0 (48)	2.5 (28)	6.2 (19)	5.2 (16)
Propanoic acid	0.1 (20)	0.5 (7)	0.1 (6)	0.2 (6)	0.9 (6)	1.3 (37)	1.2 (6)	1.7 (20)	2.7 (8)	1.5 (5)
Hydroxyacetone	0	0.1 (1)	0.1 (6)	0.1 (3)	0.6 (4)	0	0.4 (2)	0.4 (5)	3.3 (10)	2.9 (9)
Other	0.5 (60)	4.3 (64)	0.9 (50)	0.4 (11)	4.2 (30)	0.6 (17)	7.2 (38)	1.3 (15)	3.4 (10)	5.2 (16)
CO	0	1.1	0.4	0.3	0.6	1.0	10.6	1.6	2.1	3.0
CO_2	0.4	0.2	0.2	0.9	5.0	2.6	1.9	2.1	9.7	10.2
Lactic conversion (based on lactic acid recovered)	−8.4	5.7	−2.5	5.5	19.9	1.7	17.4	17.6	45.5	39.9
Lactic conversion (based on product recovered)	0.7	6.5	1.8	3.4	14.1	4.2	18.6	8.7	33.4	32.6
Carbon recovery (%)	109.1	100.8	104.3	97.8	94.2	102.4	101.2	91.1	87.9	92.7

[a] Selectivity given in parentheses.
[b] 0.3-sec residence time.

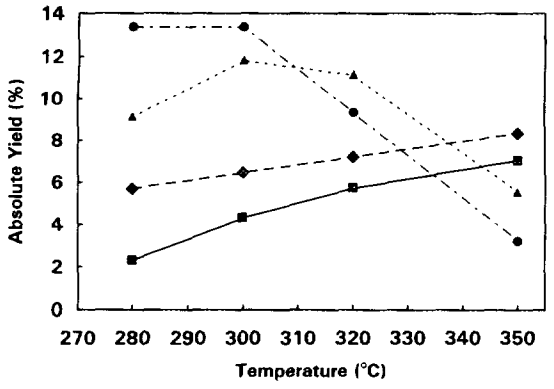

FIG. 3. 2,3-Pentanedione yield versus temperature over supported Na_3PO_4 at different contact times: 0.3 sec (■), 1.0 sec (◆), 2.0 sec (▲), and 4.0 sec (●).

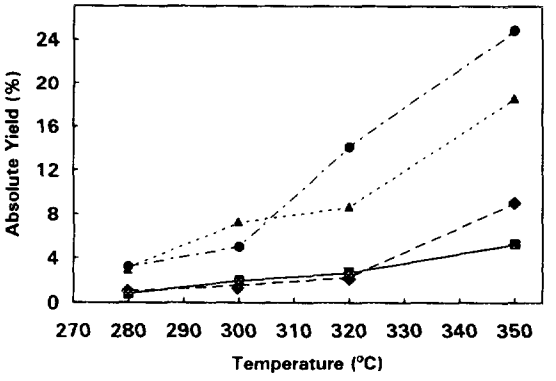

FIG. 5. Acetaldehyde yield versus temperature over Si/Al support alone and over Na_3PO_4 on Si/Al. Contact time 0.3 sec: Si/Al alone (◆), Na_3PO_4 on Si/Al (■), contact time 2.0 sec: Si/alone (●), Na_3PO_4 on Si/Al (▲).

Acetaldehyde yield over Na_3PO_4 and over the support alone (Fig. 5) increases monotonically with temperature; the slightly lower acetaldehyde yield in the presence of Na_3PO_4 above 300°C likely results from neutralization of acid sites on the Si/Al support by the basic salt. Acidic sites result in decarbonylation of lactic acid to acetaldehyde (9).

A series of experiments with different catalyst loadings showed no significant trends in activity or selectivity upon changing the loading of Na_3PO_4 on Si/Al from 4×10^{-4} to 1×10^{-3} mol/g support. Calculations indicate that there is sufficient salt present to cover the support with multiple molecular layers even at the lowest loading.

Several reactions were conducted with biomineral-derived calcium hydroxyapatite. Acrylic acid and 2,3-pentanedione yields over the hydroxyapatite are substantially lower than over the disodium and trisodium phosphates, as evidenced by Fig. 6 for an extended 100-hr run at 320°C and 4-sec residence time.

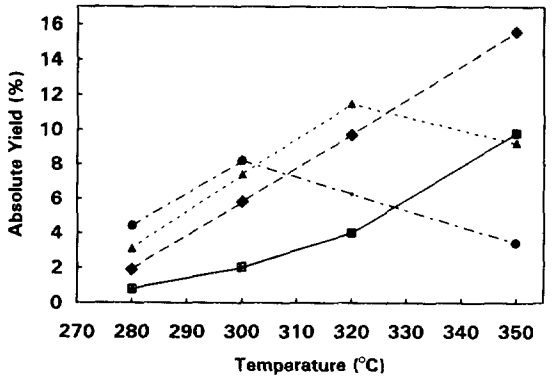

FIG. 4. Acrylic acid yield versus temperature over supported Na_3PO_4 at different contact times: 0.3 sec (■), 1.0 sec (◆), 2.0 sec (▲), and 4.0 sec (●).

Kinetic Analysis

A preliminary kinetic analysis has been carried out to identify reaction orders and kinetic parameters for the products formed over over Na_3PO_4 (Figs. 3–5). First, heats of reaction at 298 K and equilibrium constants at reaction conditions (300°C) for the primary reactions were calculated using literature values (26–29) where available or estimated using molecular orbital calculations or comparisons to similar species. The results in Table 3 show that all reaction pathways are thermodynamically favorable.

Analysis of potential mass transport resistances, using the Weiss–Prater criterion, indicated that the observable modulus $\eta\phi^2$ is less than 0.02 at all reaction conditions studied. The reaction can therefore be considered free from mass transport limitations.

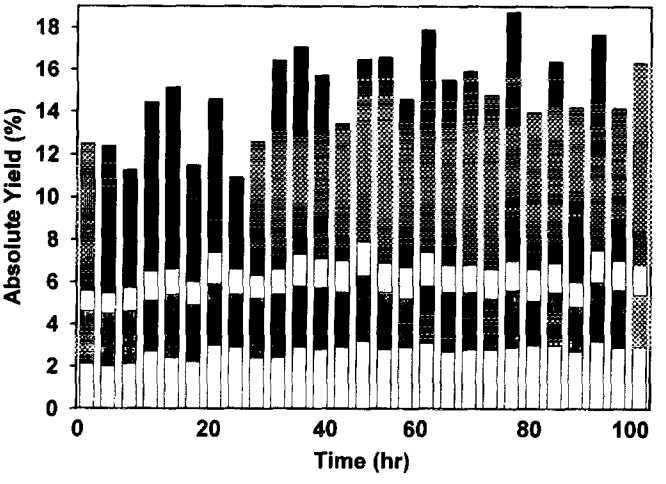

FIG. 6. Product yields versus time over calcium hydroxyapatite at 320°C and 4.0-sec contact time: acrylic acid (▩), 2,3-pentanedione (■), propanoic acid (□), hydroxyacetone (▨), other (▥), and acetaldehyde (▧).

TABLE 3

Heats of Reaction and Equilibrium Constant for Primary Reaction Pathways of Lactic Acid

Reaction	$\Delta H_{r,298\ K}$ (kj/mol)	$K_{3,573\ K}$
$CH_3CH(OH)COOH \rightarrow CH_3CHO + CO + H_2O$	87	2×10^6
$CH_3CH(OH)COOH \rightarrow CH_3CHO + CO_2 + H_2$	46	7×10^7
$CH_3CH(OH)COOH \rightarrow CH_2 = CHCOOH + H_2O$	27	8×10^3
$2\ CH_3CH(OH)COOH \rightarrow C_2H_5C(O)C(O)CH_3 + 2H_2O + CO_2$	-21^a	2×10^{8a}

[a] Estimated from molecular orbital modeling calculations.

Kinetic constants were estimated by integrating the one-dimensional molar balances for each product species in the fixed-bed reactor and estimating kinetic parameters using an in-house software package (KINFIT). Secondary decomposition of acrylic acid and 2,3-pendanedione was included as a first-order reaction to unspecified products. Results of the kinetic analysis over Na_3PO_4 on Si/Al are given in the Arrhenius plot in Fig. 7 for the three primary reaction steps. All reaction steps are first order in lactic acid except for 2,3-pentanedione formation, which is second order in lactic acid concentration. The second-order fit for 2,3-pentanedione formation was significantly better than an attempted first-order fit.

DISCUSSION

Carbon Balance

Accurate product analysis and closure of the carbon mass balance posed a challenge in this study, because numerous products are formed and because lactic acid does not easily vaporize. In addition to configuring the reactor and developing and characterizing analytical schemes to facilitate product recovery, substantial effort was made to identify additional carbon loss via other routes.

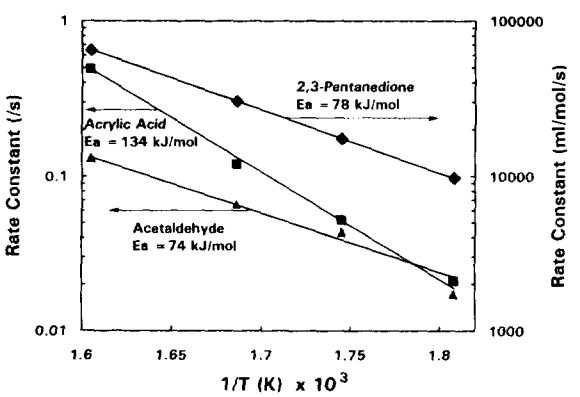

FIG. 7. Arrhenius plot for primary decomposition pathways of lactic acid. Left axis: first-order rate constants for reaction to acrylic acid and acetaldehyde. Right axis: second-order rate constant for reaction to 2,3-pentanedione.

Carbon deposition on the Si–Al support and on Na_3PO_4 on Si/Al was measured as the weight loss of dried, residual catalysts during heating in air at 550°C for 24 hr. Based on this analysis, as much as 4% of the carbon fed in lactic acid was deposited on the Si/Al support and as much as 7% was deposited on Na_3PO_4 on Si/Al. These numbers have not been included in the calculated carbon recoveries in Table 2, but they can account for a significant fraction of unrecovered carbon in many experiments.

Most of the carbon deposited was located at the top of the catalyst bed, suggesting either that unvaporized lactic acid contacts the catalyst or that coking simply occurs mainly at the top of the catalyst bed. To test the possible effect of unvaporized feed contacting the catalyst, we added a 0.5-cm layer of 1-mm nonporous glass beads on top of the catalyst. Conversion and selectivity were unaffected by the presence of this added layer, although carbon deposition was now observed on the beads but not on the catalyst. The contact of unvaporized lactic acid feed with the catalyst therefore cannot be ruled out, but we can say that this contact does not affect catalyst activity. It is apparent that catalysis occurs upon contact of vaporized lactic acid with the phosphate salts. This is supported by results of experiments in which catalyst bed depth instead of feed rate was varied as a means of altering residence time. Overall conversion and selectivity was the same for the same residence time in both of these sets of experiments, a strong indication that catalysis and not reactor morphology controls product formation.

The reproducibility of gas chromatographic analyses was tested using a number of repeated runs of a representative sample. The standard deviations of major product peak areas are between 1.5 and 7.5% of the mean peak area, while the standard deviation of lactic acid peak area is 14% of the mean area. Product yields are therefore reliable and do not contribute substantially to uncertainty in the mass balance. On the other hand, analysis of lactic acid recovery, especially at low conversion, can contribute to uncertainty in the carbon balance.

The extended 100-hr run (320°C, 5-sec residence time) with hydroxyapatite catalyst (Fig. 6) gives further evidence of the reliability of product analysis. Relatively stable product yields were achieved, and the average carbon recovery for the 27 samples taken during the run was 102.4% with a standard deviation of 8.2%. No measurable carbon deposition occurred on the catalyst during the run.

Formation of 2,3-pentanedione

The formation of 2,3-pentanedione from lactic acid was an unexpected and heretofore unknown reaction pathway. Our discovery of this pathway came about because we conducted reactions at higher pressure (0.5 MPa) and lower temperatures (280–320°C) than in previous studies of lactic acid conversion, where conditions (0.1 MPa, 350–400°C) were set to maximize acrylic acid yields. Our kinetic analysis indicates that 2,3-pentanedione formation is second order in lactic acid and thus should be favored at elevated pressures. The effect of pressure on 2,3-pentanedione yield is currently under investigation in our laboratories.

Because propanoic acid and acetaldehyde are both products of lactic acid conversion, we tested the possibility that the pentanedione might arise via a condensation between these fragments, with loss of water. Alternatively, pentanedione might be the primary product which gives rise to the two low-molecular-weight species via hydrolytic fragmentation. However, none of these three compounds, individually or in combination, reacted significantly over supported Na_3PO_4 catalyst at temperatures up to 350°C and 1.5-sec residence time, conditions under which lactic acid is significantly converted to acetaldehyde, propanoic acid, and pentanedione.

Two possible mechanisms for condensation of lactic acid to 2,3-pentanedione are shown in Fig. 8. The essential elements of these two pathways are similar. The phosphate combines with the acyl group of lactic acid to form a carboxylic phosphoric anhydride (or acyl phosphate) as shown in mechanism (a). Although it is not required by the mechanism, the hydroxyl group on C2 of the lactic acid may also form an ester linkage with the phosphate group to give a cyclic structure [mechanism (b)]. In either case, the β-proton of the now activated lactic acid is abstracted by base to give a resonance-stabilized enolate anion. This carbon nucleophile then attacks the carbonyl carbon of another molecule of acyl phosphate, displacing the phosphate group. The resulting C6 species then decarboxylates (→C5) and rearranges to 2,3-pentanedione. This latter rearrangement is precedented in the base-catalyzed rearrangement of 1,3-dihydroxy-2-propanone (dihydroxyacetone) to pyruvaldehyde (30). The overall stoichiometry is supported by the correlation between 2,3-pentanedione and CO_2 yields (Table 2).

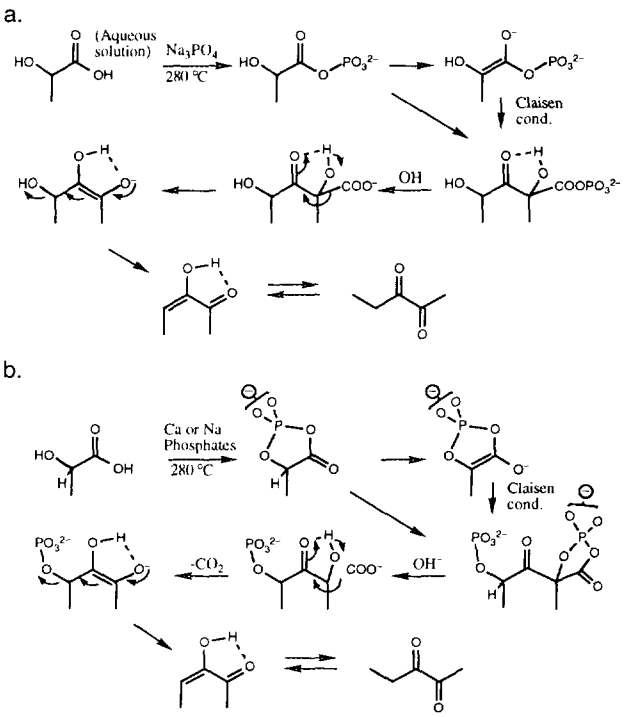

FIG. 8. Two proposed mechanisms for 2,3-pentanedione formation from lactic acid over phosphate catalysts: (a) reaction of acyclic carboxylic phosphoric anhydride form; (b) reaction of cyclic anhydride form.

If the proposed mechanism (Fig. 8) represents a general pathway for conversion of α-hydroxy carboxylic acids to α-diketones, then, for example, 2-oxo-propanal (pyruvaldehyde) should be formed from 2-hydroxyacetic (glycolic) acid, and 2,3-butanedione or 2-oxo-butanal should arise from glycolic acid/lactic acid mixtures. We therefore fed glycolic acid (28.7 wt% in solution, Aldrich) at 280°C and 0.3–1.5-sec residence time over Na_3PO_4 on Si/Al. No 2-oxo-propanadehyde was found in the reactor effluent; glycolic conversion was less than 5% and the only product of note was a trace amount of 2,3-butanedione. In a second experiment, an aqueous solution of 20.0 wt% lactic acid and 14.4% glycolic acid was reacted under conditions identical to those used in the experiment with glycolic acid. This mixture produced no 2-oxo-butanaldehyde and a quantity of 2,3-butanedione similar to that formed from glycolic acid alone.

In retrospect, the fact that glycolic acid fails to form α-dicarbonyl condensation products can be rationalized in terms of the mechanism in Fig. 8. The methyl substituent in the lactic acid favors enolate formation, which is the key process leading to C–C bond formation between previously separate subunits. Thus, the absence of the methyl group in glycolic acid impedes the condensation pathway. Finally, we were unable to test our hypothesis on higher molecular weight α-hydroxy carboxylic acids because they are nonvolatile compounds.

Product Yields and Pathways

Results in Table 2 show that the primary pathway of lactic acid decomposition over the acidic silica–alumina support is decarbonylation to acetaldehyde and CO. When phosphate salts are loaded onto the support, this pathway is strongly inhibited and the smaller amount of acetaldehyde formed is mainly via decarboxylation (to give CO_2). As supported by Sawicki (9) in vapor phase studies and by Mok *et al.* (18) in supercritical water experiments, it is clearly desirable to maintain basic conditions to avoid acetaldehyde formation via decarbonylation.

Decarboxylation also produces hydrogen, which has been shown to react with acrylic acid to form propanoic acid (18). Although the data suggest a relationship between the extent of decarboxylation and formation of propanoic acid, at this time our product yield calculations are not precise enough to attempt to correlate the two. A further complication is that propanoic acid apparently also forms via contact of lactic acid with metal parts of the reactor: our initial experiments, before we installed a quartz liner in the reactor, resulted in high yields of propanoic acid. Although there is now no contact of reactants with metal parts in the high-temperature region of the reactor, the reactor exit tube is 304 stainless steel and could facilitate some formation of propanoic acid at lower temperatures. Regardless of its source, the yield of propanoic acid is low in most reactions we conducted.

The mechanism by which phosphate salts catalyze dehydration of lactic acid to acrylic acid is not well understood. In contrast to earlier studies (15–17) in which phosphate is postulated to stabilize the carboxylate group and thus prevent acetaldehyde formation, we propose that the phosphate forms a cyclic transition state with the C_2 and C_3 carbons via which dehydration occurs. This cyclic structure is analogous to the generally accepted transition state for elimination of acetic acid from methyl α-acetoxypropionate to form methyl acrylate (20, 21), which results in high selectivity to acrylate (>90%). Using AM1 semiempirical molecular orbital calculations, we have estimated structures and energetics for transition states of both phosphoric acid and acetic acid eliminations. As shown in Fig. 9, the low calculated activation barrier for formation of the phosphate analog suggests that such a transition state is formed and is the primary route to acrylic acid formation.

It is noteworthy that monosodium phosphate [as $(NaPO_3)_n$] shows little catalytic activity for acrylic acid formation relative to the di- and trisodium salts. The more basic salts, which in their active forms possess at least two sodium atoms per phosphorus, may be more able to form the proposed cyclic structures required for acrylic acid formation.

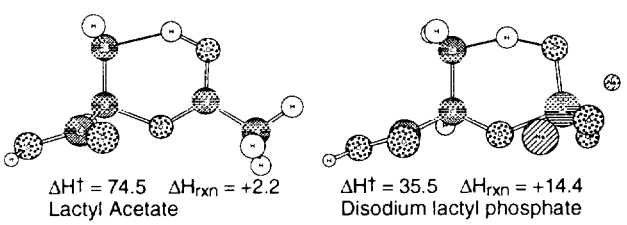

FIG. 9. Transition structures for cycloeliminations of acetic acid (left) and Na_2HPO_4 (right) from their lactic acid esters. Calculated activation and reaction enthalpies (kcal/mol) are shown below structures.

CONCLUSIONS

Lactic acid is converted to acrylic acid, 2,3-pentanedione, and acetaldehyde over supported sodium phosphate salts at 0.5 MPa and 280–350°C. Formation of 2,3-pentanedione is favored at low temperatures (280°–320°C) and longer residence times, while acrylic acid is favored at higher temperatures (350°C) and shorter residence times. Yields and selectivities of 2,3-pentanedione and acrylic acid reported here are not optimal, because initial studies have been conducted at relatively low lactic acid conversions to avoid secondary reactions.

We propose that 2,3-pentanedione is formed by a second-order condensation pathway in the presence of phosphates; this mechanism is supported by the correlation between yields of CO_2 and 2,3-pentanedione. For acrylic acid formation, we propose a cycloelimination pathway through which phosphate is cleaved from lactic acid–2-phosphate to form acrylic acid. Disodium and trisodium phosphate are more effective catalysts than the monosodium salt, because they have the mobility and structure which facilitate formation of the required intermediate. Future work will focus on enhancing desirable product yields as well as further clarifying mechanistic aspects of this reaction system.

ACKNOWLEDGMENTS

The support of the Crop and Food Bioprocessing Center (State of Michigan Research Excellence Fund) and the Michigan Biotechnology Institute is gratefully acknowledged. JEJ also thanks Amoco Oil Company for early support of studies on catalytic dehydration. Doug Wadley and Robert Langford conducted several of the experiments related to reactor characterization and carbon mass balances.

REFERENCES

1. Lipinsky, E. S., and Sinclair, R. G., *Chem. Eng. Prog.* **82**(8), 25 (1986).
2. Keeler, R., *Res. Dev. February*, 52 (1991).
3. Fisher, C. H., and Filachione, E. M., U.S. Dept. Agr., Bur. Agr. and Ind. Chem. AIC-279 (1950).
4. Holmen, R. E., U.S. Patent 2,859,240 (1958).
5. Nakel, G. M., and Dirks, B. M., U.S. Patent 3,579,353 (1971).
6. Maresca, L. M., U.S. Patent 4,611,033 (1986).
7. Matsumoto, T., Yamada, E., Nakachi, O., and Komai, T., Japanese Patent 61,243,807 (1986); (CA 106:138889k).

8. Paparizos, C., Dolhyj, S., and Shaw, W. G., U.S. Patent 4,786,756 (1988).
9. Sawicki, R. A., U.S. Patent 4,729,978 (1988).
10. Walkup, P. C., Rohrmann, C. A., Hallen, R. T., and Eahin, D. E., PRAI U.S. 90-468704 (1991); (CA 116:5328m).
11. Mercados Quimicos Industriales S.A., Spanish ES 515,891 (1983); (CA 103:124071p).
12. Hashimoto, M., and Honda, T., German Offen. DE 3,141,173 (1982); (CA 98:71498c).
13. Moffat, J. B., *Catal. Rev.-Sci. Eng.* **19**(2), 199 (1978).
14. Monma, H., *J. Catal.* **75,** 200 (1982).
15. Paecht, M., and Katchalsky, A., *Israel J. Chem.* **1,** 463 (1963).
16. Daniel, C., U.S. Patent 4,410,729 (1983).
17. Watkins, W. C., U.S. Patent 3,917673 (1975).
18. Mok, W., Antal, M. J., Jr., and Jones, M., *J. Org. Chem.* **54,** 4596 (1989).
19. Lira, C. T., and McCrackin, P. J., *Ind. Eng. Chem. Res.* **32,** 2608 (1993).
20. Burns, R., Jones, D. T., and Ritchie, P. D., *J. Chem. Soc.*, 400 (1935).
21. Smith, L. T., Fisher, C. H., Ratchford, W. P., and Fein, M. L., *Ind. Eng. Chem.* **36,** 229 (1944).
22. Greenfield, S., and Clift, M., "Analytical Chemistry of the Condensed Phosphates." Pergamon, New York, 1975.
23. Van Wazer, J. R., *in* "Kirk-Othmer Encyclopedia of Chemical Technology," 2nd ed. (H. F. Mark, J. J. McKetta, Jr., and D. F. Othmer, Eds.), Vol. 15, p. 232. Interscience, New York 1976.
24. Hayashi, S., and Hayamizu, K., *Bull. Chem. Soc. Jn.* **62,** 3061 (1989).
25. Gunter, G. C., Ph.D. Dissertation, Michigan State University, East Lansing, Michigan, 1994.
26. Lide, D. R., Ed., "CRC Handbook of Chemistry and Physics," 72nd ed. CRC Press, Boca Raton, FL, 1992.
27. Domalski, E. S., *J. Chem. Phys. Ref. Data* **1**(2), 221 (1972).
28. Thauer, R., Jungerman, K., and Decker, K., *Bacteriol. Rev.* **41,** 100 (1977).
29. Wilhoit, R., Chao, J., and Hall, K., *J. Chem. Phys. Ref. Data* **14**(1), 1 (1985).
30. Bernhauer, K., and Gorlich, B., *Biochem. Z.* **212,** 462 (1929).